

Generation of short-pulse VUV and XUV radiation

B. WELLEGEHAUSEN, H. WELLING, C. MOMMA,
M. FEUERHAKE, K. MOSSAVI, H. EICHMANN

*Institut für Quantenoptik, Universität Hannover, Welfengarten 1, 30167
Hannover, Germany*

Received 26 September 1994; revised and accepted 10 April 1995

Starting from intense short-pulse KrF (248 nm, 25 mJ, 400 fs), ArF (193 nm, 10 mJ, ~1 ps), and Ti:sapphire (810 nm, 100 mJ, 150 fs) laser systems, schemes for the generation of fixed-frequency and tunable VUV and XUV radiation by nonlinear optical techniques are investigated. With the KrF system, a four-wave mixing process in xenon yields tunable radiation in the range of 130–200 nm with output energies of, so far, 100 μ J in less than 1 ps. For the XUV spectral range below 100 nm, nonperturbative high-order harmonic generation and frequency mixing processes in noble gas jets are considered. To achieve tunability, the intense fixed-frequency pump laser radiation is mixed with less intense but broadly tunable radiation from short-pulse dye lasers or optical parametric generator–amplifier systems. In this way, tunability down to wavelengths of less than 40 nm has been demonstrated.

1. Introduction

The generation of coherent radiation in the VUV spectral range below 200 nm or in the XUV range starting below 100 nm is of interest for a variety of potential scientific and technical applications [1]. Although great efforts have been and are still being undertaken to develop primary laser sources in this spectral range, only very few laboratory soft x-ray laser systems exist so far [1, 2], and the shortest wavelengths of commercial VUV systems are still the discharge-pumped ArF (193 nm) and F₂ (157 nm) excimer lasers. Even if more laboratory laser systems at short wavelengths become available in the future, these systems will not be tunable, which will limit scientific use in particular. In order to cover broad spectral ranges in the VUV and XUV, therefore, nonlinear optical techniques have to be used, and as a result of recent progress in the realization of compact high-peak-power pump laser systems, interesting new perspectives for these techniques have been developed.

With conventional nanosecond pump sources and power levels typically in the megawatt range, only third-order and fifth-order nonlinear processes are of practical interest. Using four-wave sum- and difference-frequency mixing schemes and favourable two-photon resonances, tunable radiation down to about 70 nm has been achieved with output power levels in the 1 W range at wavelengths below 100 nm [3–6]. These sources are well developed and widely used, mostly for linear spectroscopic experiments [7]. Recently experiments have been reported with narrowband tunable radiation around 58 nm generated by fifth-order

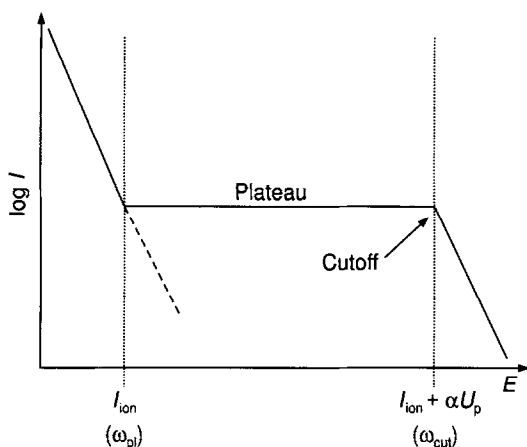


Figure 1 Schematic trend of a harmonic power spectrum, with plateau and cutoff. In perturbative nonlinear optics the harmonic power decreases continuously (dashed line).

processes [8]. To reach shorter wavelengths and also higher output powers, higher-order nonlinear processes and much higher peak powers of the pump sources have to be used. Systems suitable for this are short-pulse (ps–fs) laser systems at gigawatt power levels, which, when focused, allow intensities well above $10^{13} \text{ W cm}^{-2}$. At these intensities, corresponding to electric field strengths above 10^8 V cm^{-1} , the optical interaction is no longer a small perturbation, resulting in a dramatic change of the nonlinear response as indicated by the schematic diagram of a typical harmonic power spectrum in Fig. 1. After an initial steep (perturbative) decrease of the power for the low-order harmonics, a plateau region is reached which extends up to high harmonics, until finally at a characteristic cutoff frequency a strong decrease again follows.

With high-intensity Nd:glass, Ti:sapphire, dye and KrF excimer laser systems, harmonic generation has been studied [9–12] and harmonics up to orders of 143 and shortest wavelengths around 7 nm have been demonstrated [13]. Thus, with high-intensity pump sources, new aspects in nonlinear optics open up.

In this contribution different approaches to the generation of powerful and tunable short-pulse radiation in the VUV and XUV spectral ranges will be described and briefly discussed. For the experiments, the commercial KrF (25 mJ, 400 fs; Laser Lab. Göttingen; Lambda Physik) and Ti:sapphire (100 mJ, 150 fs; B.M. Industries) laser systems described below were used. With a near-resonant four-wave mixing process in xenon [14], tunable subpicosecond radiation in the range of about 130–200 nm can be generated with output powers exceeding $100 \mu\text{J}$; and using high-order mixing processes, tunability down to less than 40 nm has been demonstrated.

2. Pump laser systems

The short-pulse pump laser systems at 248 nm (KrF) and at about 810 nm (Ti:sapphire) are shown schematically in Figs 2 and 3. In both systems, short pulses generated by suitable oscillators are amplified to higher energies.

The excimer system (Fig. 2) consists of a standard double-discharge tube excimer laser (EMG 150; Lambda Physik), in which one discharge channel is operated as a 20-ns oscillator at 308 nm (XeCl) and the other as an amplifier at 248 nm (KrF). Because excimer lasers cannot directly generate short pulses, femtosecond pulses at 496 nm ($2 \times 248 \text{ nm}$) are first generated by a specially designed dye laser chain [15], pumped by the 308 nm radiation from the XeCl

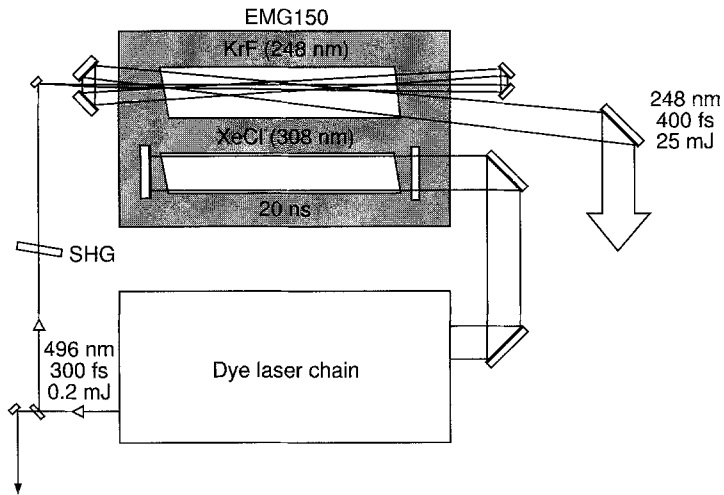


Figure 2 Short-pulse KrF excimer laser system.

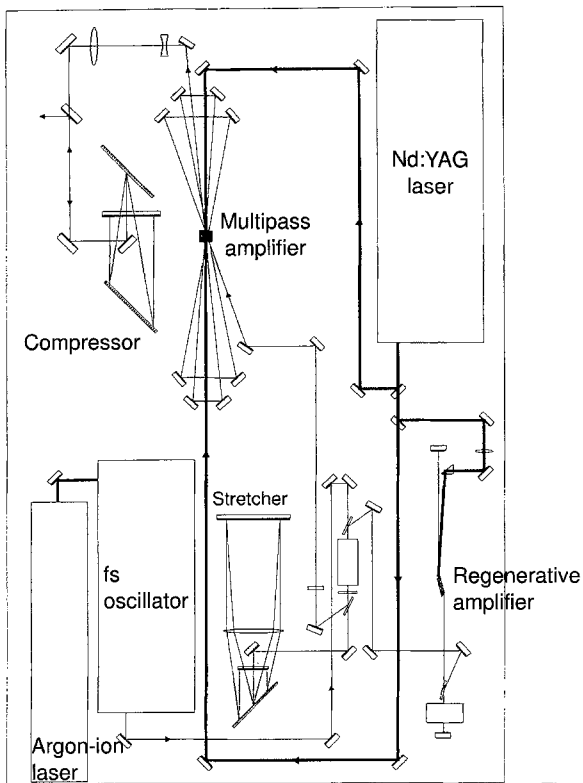


Figure 3 High-power Ti:sapphire laser system.

oscillator. This chain finally delivers at 496 nm pulses with a duration of 300 fs at an energy of about 200 μJ . After frequency doubling, 248 nm pulses are obtained which are then amplified in the amplifier channel. With a three-pass off-axis amplification geometry [16], pulses with an energy up to 25 mJ in about 400 fs and a quadratic beam shape ($\sim 3 \times 3 \text{ cm}^2$ at the exit window) are obtained. The pulses are not Fourier limited and may be further compressed [15]. In addition to the 248 nm radiation, powerful pulses of about 100 μJ at 496 nm after the frequency doubler may also be used for nonlinear optical experiments.

The Ti:sapphire laser system uses the chirped-pulse amplification (CPA) technique [13] to generate pulses at the terawatt power level. A CW mode-locked Ti:sapphire oscillator (Coherent Mira) first generates a continuous train of 150 fs pulses (repetition rate $\sim 80 \text{ MHz}$) at an average energy of about 1 W. These pulses are stretched to about 200 ps and then a single pulse is subsequently amplified in Ti:sapphire amplifier crystals pumped by the second harmonic of a powerful Nd:YAG laser (1 J, 10 ns, repetition rate 10 Hz). Amplification is first performed in a regenerative amplifier up to pulse energies of $\sim 8 \text{ mJ}$ and then in a six-pass amplifier to, presently, about 200 mJ. After final pulse compression the system delivers a beam (diameter $\sim 2 \text{ cm}$) with energy up to 100 mJ in 150 fs. The pulses are almost Fourier limited.

3. Four-wave mixing in xenon

For the generation of tunable VUV radiation a near-resonant four-wave mixing process in xenon is used [14]. By excitation of xenon with the KrF short-pulse radiation near the $5p^6$ – $6p$ two-photon resonance (Fig. 4) at intensities of about $10^{13} \text{ W cm}^{-2}$, a strong nonlinear polarization is generated, which can start intense parametric oscillations. For the tunable VUV generation, in addition, a tunable visible to near infrared laser field has to be injected, as indicated in Fig. 4. Phase matching can be accomplished by a noncollinear mixing geometry [14]. With nanosecond tunable pulses in the range of 350 nm to $2 \mu\text{m}$, tunable subpicosecond VUV radiation in the range of ~ 200 – 130 nm has been demonstrated [17]. Nanosecond pulses can be used to generate short VUV pulses, because the two-photon polarization induced by the KrF laser is short-living. However, it is more favourable to use subpicosecond tunable radiation directly derived from the main pump system, in order to avoid problems due to the synchronization of independent sources. Therefore, distributed feedback or travelling-wave

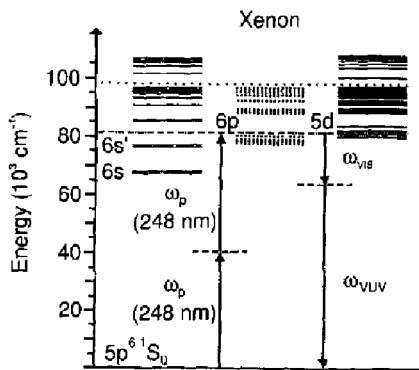


Figure 4 Xenon level scheme with near-resonant parametric four-wave mixing.

dye lasers, pumped by a fraction of the short-pulse 496 nm or 248 nm radiation from the system, have been developed [18], which allow the generation of subpicosecond pulses in the 350–600 nm range with energies of several microjoules. Figure 5 shows examples where these pulses have been used to generate VUV radiation at wavelengths around 193 nm and 157 nm, respectively. Pulses at these wavelengths have been used to study the short-pulse amplification characteristics of discharge-excited ArF (193 nm) and F₂ excimer amplifiers [19, 20]. At the ArF wavelength, pulses of about 1 ps with energies up to 10 mJ could be generated in this way. This radiation has been used in frequency mixing experiments described below.

In the mixing process considered, both radiation fields ω_{vis} and ω_{VUV} are exponentially amplified in the small-signal regime. From investigations of the self-starting four-wave

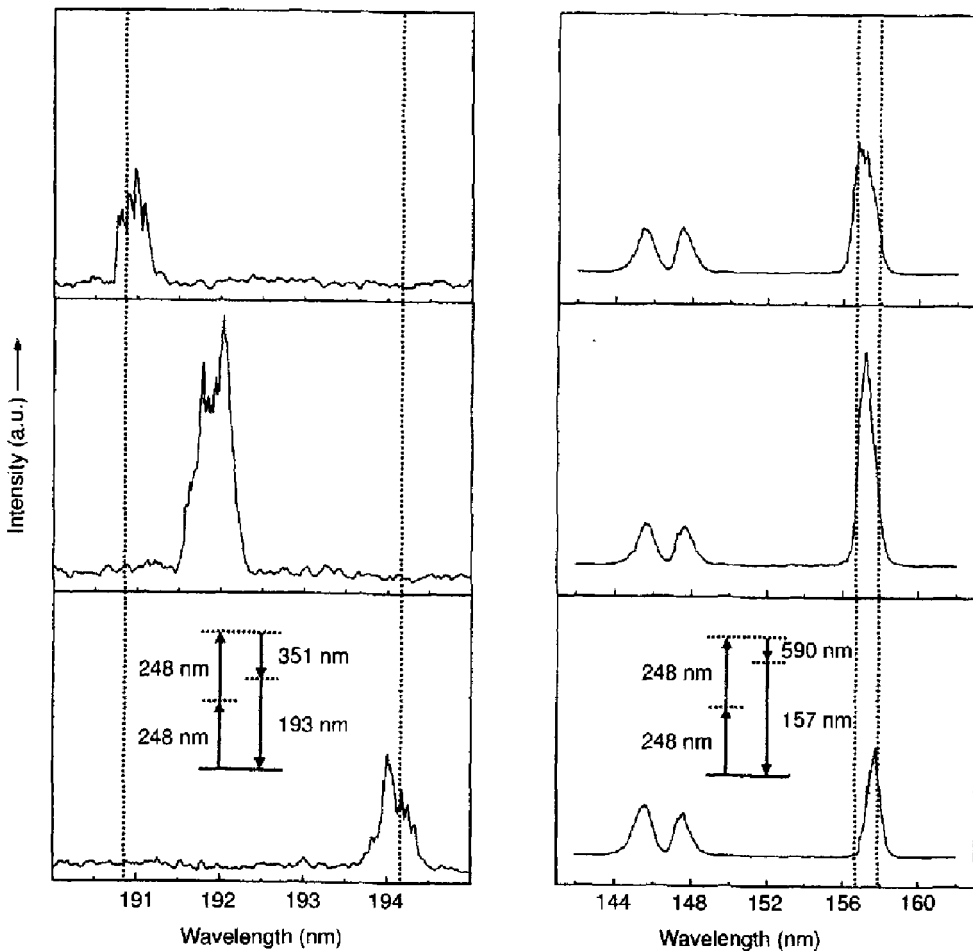


Figure 5 Spectra of generated VUV radiation tuned around 193 nm and 157 nm. Pump energy (248 nm) 5 mJ (400 ps, 10^{13} – 10^{14} W cm⁻²). With about 80 μ J at 351 nm (≤ 2.5 ps) and 3 μ J at 590 nm (400 fs), about ~ 5 μ J at 193 nm (< 1 ps) and 3 μ J at 157 nm (< 1 ps) are generated. The emission around 146 nm is due to a self-starting four-wave parametric oscillation process (see [14]).

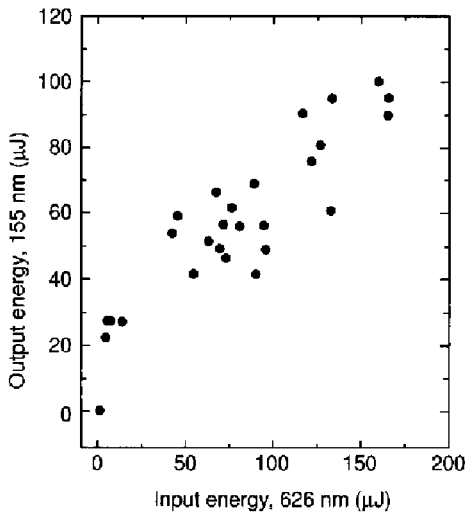


Figure 6 Energy of short-pulse VUV radiation at 155 nm versus energy of the visible input radiation at 626 nm. Pump energy (248 nm) is 11 mJ.

parametric generation process in xenon [14] it is known that tremendous amplifications are possible, so that fields with macroscopic output energies can build up from noise, as can be seen from the emission around 146 nm in Fig. 5. At higher energies of the fields, the amplification will saturate, and in this regime it can be expected that the energy E_{VUV} of the VUV field increases proportional to the energy E_{vis} of the visible input field and reaches comparable values. This can already be seen from the data of Fig. 5. To further increase the VUV energy, mixing experiments at higher energies of the visible input field have been performed, which are summarized in Fig. 6. With up to 180 μJ input radiation at 626 nm (330 fs), a maximum VUV energy of 100 μJ has been achieved so far for about 11 mJ of pump radiation at 248 nm. As can be seen from Fig. 6, at low 626 nm input energies the VUV energy increases strongly and then turns over to an almost linear increase. The 626 nm short-pulse radiation was generated by Raman shifting (first Stokes in hydrogen) of the 496 nm radiation from the main excimer pump laser system (see Fig. 2) and subsequent amplification in dye solutions pumped by 2ω of a Nd:YAG laser. Because no saturation can be seen in the present experiments, it is expected that short-pulse tunable VUV radiation around 160 nm with energies approaching the 0.5 mJ level and gigawatt powers for subpicosecond pulses will be possible, which should be of interest for applications including further nonlinear frequency conversion into the XUV. For the future it is planned to generate the tunable short-pulse input radiation by use of tunable optical parametric generator–amplifier (OPG) schemes.

4. Fixed frequency harmonic generation

For the generation of short-pulse radiation in the XUV spectral range, higher-order nonlinear processes have to be used when starting from presently available high-power short-pulse pump laser systems. With KrF and ArF lasers, frequency tripling will lead to radiation of 83 nm and 64 nm and with fifth-order harmonics 50 nm and 39 nm can already be reached, whereas, with Ti:sapphire lasers at 800 nm, harmonics of the order 9 up to 21 have to be considered. Therefore, intuitively the short-wavelength systems seem to be favoured, which is true in the perturbative regime of nonlinear optics. However, at high pump intensities this situation changes, as indicated by the schematic harmonic response curve in Fig. 1. This nonperturbative

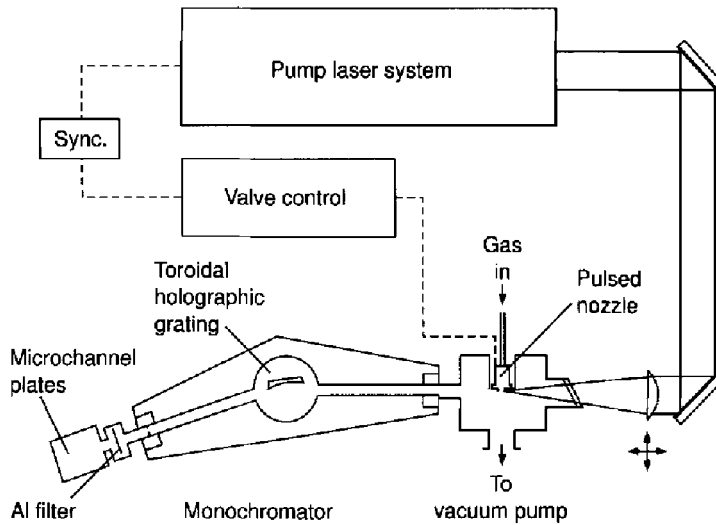


Figure 7 Experimental setup for the generation and detection of XUV radiation.

response is characterized by two frequencies. A lower frequency ω_{pl} where the plateau starts, and a cutoff frequency ω_{cut} where the plateau ends. The energy $\hbar\omega_{pl}$ corresponds to the ionization potential I_{ion} of the nonlinear material, while the cutoff energy is given by $\hbar\omega_{cut} = I_{ion} + \alpha U_p$ [21], with $U_p = (e^2/2\epsilon_0 m_e c) I_p / \omega_p^2$ being the ponderomotive potential; ω_p is the pump laser frequency and I_p the pump intensity of the laser up to the limit of the saturation intensity I_{sat} [22]. Theoretically, the factor α is 3.2 (single-atom response) [23], while experimentally α values in the range of 2–3 have been observed [22, 24]. The $1/\omega_p^2$ dependence of the cutoff frequency therefore favours longer-wavelength pump lasers for shorter wavelength generation. However, with shorter-wavelength pump lasers, higher efficiencies at lower orders can be expected.

To test this behaviour, harmonic generation with short-pulse KrF, ArF and Ti:sapphire laser radiation has been compared. The basic experimental setup for this and for frequency mixing experiments described later is shown in Fig. 7. The pump radiation is focused into a gas jet emerging from a pulsed nozzle into a vacuum chamber. The XUV radiation generated is analysed down to about 10 nm by an XUV monochromator (Yobin Ivon LHT 30) and detected by a microchannel plate detector (Galileo, $d = 3.2$ cm). For the experiments, noble gases and hydrogen were used. At backing pressures of the nozzle in the range of several bars, vapour pressures in the jet of several tens of millibars are reached, as determined experimentally. The gas jet had a thickness of about 1 mm at the working distance immediately behind the nozzle exit.

Figures 8 and 9 show examples of harmonic spectra for KrF in helium and for Ti:sapphire in neon, and Figs 10–12 summarize the data obtained. For ArF only the fifth harmonic could be observed in argon; for KrF up to the 11th harmonic in helium; and for Ti:sapphire in neon so far the 71st harmonic at 11 nm, the limit of the detection system. In the literature, for Ti:sapphire and KrF harmonics up to orders of 109 [10] and 25 [12] have been reported, whereas for ArF no higher harmonics than the fifth have been seen so far [25].

For the interpretation of the dependences, the data and parameters summarized in Table I are helpful. The ionization potential defines the plateau wavelength λ_{pl} (ω_{pl}). With increasing ionization energy, from the heavy to the light noble gases, the polarizability and consequently

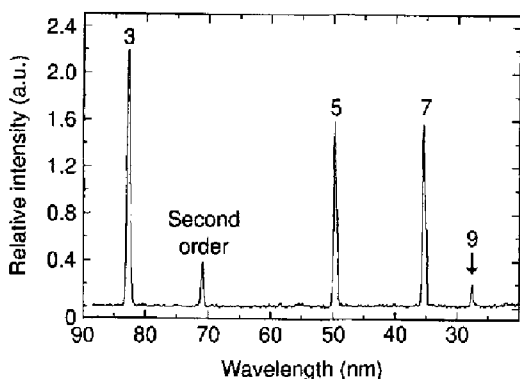


Figure 8 Harmonic spectrum of KrF (248 nm) pump radiation in helium. Pump intensity $\sim 10^{16} \text{ W cm}^{-2}$. The spectrum is not corrected with respect to the monochromator and detector characteristics.

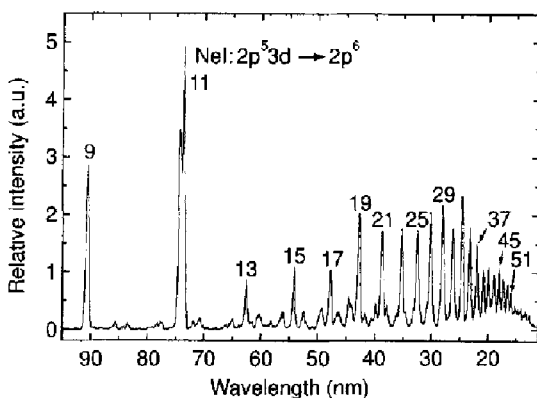


Figure 9 Harmonic spectrum of Ti:sapphire (810 nm) pump radiation in neon. The spectrum is not corrected. The signals between the marked harmonics are due to the second grating order of the monochromator.

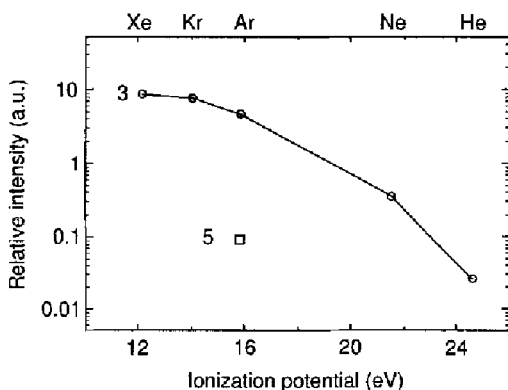


Figure 10 Intensity of third- and fifth-order harmonics of 193 nm radiation (ArF, intensity $\sim 10^{15} \text{ W cm}^{-2}$) for different noble gases (ionization potentials).

the harmonic power decreases. This can be seen clearly from the data in Fig. 10 for the third harmonic of ArF. To see whether a plateau is possible and to estimate the cutoff wavelength λ_{cut} , the ponderomotive potential U_p has to be determined. As discussed above, the intensity in the equation for U_p is limited by the saturation intensity I_{sat} , which is the intensity where

TABLE I

Pump laser:	KrF (248 nm)					ArF (193 nm)					Ti:sapphire (810 nm)				
	Xe	Kr	Ar	Ne	He	Xe	Kr	Ar	Ne	He	Xe	Kr	Ar	Ne	He
I_{ion} (eV)	12.1	14	15.8	21.6	24.6	12.1	14	15.8	21.6	24.6	12.1	14	15.8	21.6	24.6
I_{sat} (10^{14} W cm $^{-2}$)	1.2	1.4	3.6	11.4	16.7	0.3	1.7	2	6.5	12.9	1	1.4	2	4.8	7
$U_p(I_{\text{sat}})$ (eV)	0.7	0.8	2.1	6.6	9.6	0.1	0.6	0.7	2.3	4.5	5.8	8.6	12.2	29.4	42.8
$I_{\text{ion}} + 2U_p$ (nm)	92	79	62	36	28	101	82	72	47	37	52	40	31	15	11

The saturation intensity I_{sat} was calculated using multiphoton ionization for the excimer lasers (KrF, ArF) and tunnelling ionization for the Ti:sapphire laser.

strong ionization occurs, due to multiphoton or field ionization. Multiphoton ionization is more probable for shorter pump laser wavelengths and lower ionization potentials, corresponding to a Keldysh parameter [26] $\gamma \gg 1$, whereas field ionization is the dominant mechanism for long wavelength lasers and media with high ionization potentials ($\gamma < 1$). Estimated values for I_{sat} , $U_p(I_{\text{sat}})$ and λ_{cut} are given in Table I.

From Table I it can be seen that for the ArF laser the cutoff wavelength for argon as non-linear medium is below the third harmonic wavelength. Therefore, a plateau, or at least higher harmonics, cannot be expected for the heavier noble gases, which is in agreement with the experimental result that only the fifth harmonic has been detected in argon. Owing to the lower polarizability of the lighter elements neon and helium, the signals at the fifth-order harmonics were too weak to be distinguishable from the background. For the KrF laser a plateau should be possible for neon and helium as nonlinear medium, but a plateau-like feature could only be seen in helium (Fig. 11), with an estimated cutoff corresponding to an α -value of approximately 2.

Sarukura *et al.* [12] have observed harmonics up to the 25th order in helium (9.9 nm) with the KrF radiation at intensities up to 10^{18} W cm $^{-2}$, which is far above the estimated cutoff wavelength and contradicts our observations. As already pointed out by Krause [21], it is believed that these high harmonics arise from ions produced by the high-intensity laser field.

With the Ti:sapphire system clear plateaux and well-defined cutoffs have been observed (Fig. 12). The energetic positions of the cutoffs for the different noble gases and at pump intensities above the corresponding saturation intensities are in good agreement with the calculated values from Table I, assuming an α -value of 2.3. For the heavier noble gases xenon, krypton and

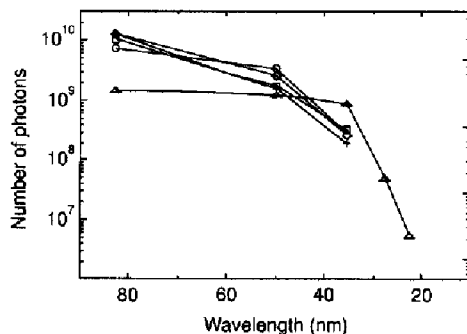


Figure 11 Measured photon numbers of 248 nm (KrF, $\sim 10^{18}$ W cm $^{-2}$) harmonic radiation for different noble gases: \diamond , xenon; +, krypton; \square , argon; \circ , neon; Δ , helium. For the third harmonics the photon numbers correspond to energies of 3–30 nJ and peak powers of 3–30 kW assuming a pulse duration of 1 ps.

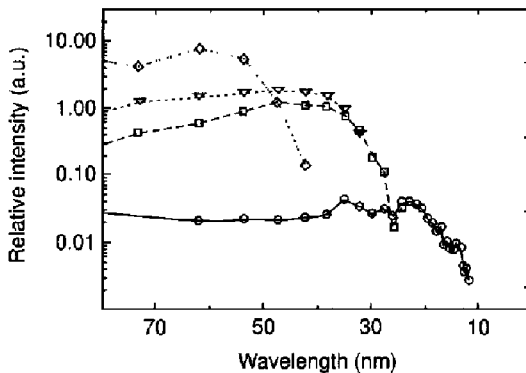


Figure 12 Harmonic intensities of Ti:sapphire (810 nm, ~50 mJ) radiation for different noble gases: \diamond , xenon; ∇ , krypton; \square , argon; \circ , neon.

argon, this result is in good agreement with detailed theoretical and experimental investigations from Wahlström and L'Huillier, respectively [22, 24]. The observed cutoff for neon is not real and is caused by the strong decrease of the sensitivity of the detection system at wavelengths below 12 nm. For helium as nonlinear medium the intensity of the harmonics was too weak for an unambiguous separation from noise.

Absolute photon numbers have been measured for the harmonics of the excimer laser radiation using a calibrated XUV semiconductor photodiode (UDT X-UV 20). The stated sensitivity of the diode agrees in the visible spectral range within a factor of 2 with measured values, using subpicosecond pulses at 496 nm.

As shown in Fig. 11, at the third harmonics of the KrF system, photon numbers of the order of 10^9 to 10^{10} have been measured. For the Ti:sapphire laser such absolute measurements have not been performed until now, but in [22] photon numbers of 10^8 – 10^9 at 60 nm for optimum conditions (long confocal parameter) have been determined, which are about one order of magnitude smaller than for the KrF pump radiation for our experimental conditions. However, at wavelengths below about 20 nm, harmonics from the longer-wavelength lasers seem to be more powerful [27].

The present power of the harmonics already corresponds to peak brightnesses which are several orders of magnitude higher than those of synchrotron sources in this spectral range [28]. Therefore, high harmonics may be an alternative, compact, and easy to realize source, especially for those applications that require high peak powers of short pulses.

5. Generation of tunable XUV radiation by high-order frequency mixing

For many applications tunable XUV radiation is desirable and, in principle, can be realized by the harmonic generation process if tunable pump lasers are used. Among the high peak power sources, only Ti:sapphire is sufficiently tunable. However, tuning of a terawatt laser system as shown in Fig. 3 is difficult, because the oscillator and the whole pulse chirping and compression units have to be adjusted. Therefore, it is more practicable to mix the radiation of a high-power fixed-frequency laser system (ω_p) with a less powerful but easily tunable light source (ω_{tun}) to generate tunable radiation at $n\omega_p \pm k\omega_{\text{tun}}$ ($n+k$ odd) by high-order frequency mixing. Such mixing experiments have been performed with the ArF and KrF excimer radiation and the KrF and 496 nm dye laser radiation at fixed frequencies, and with the Ti:sapphire laser and a tunable OPG system to generate tunable XUV radiation.

The experimental setup for the frequency mixing experiments is similar to that for harmonic

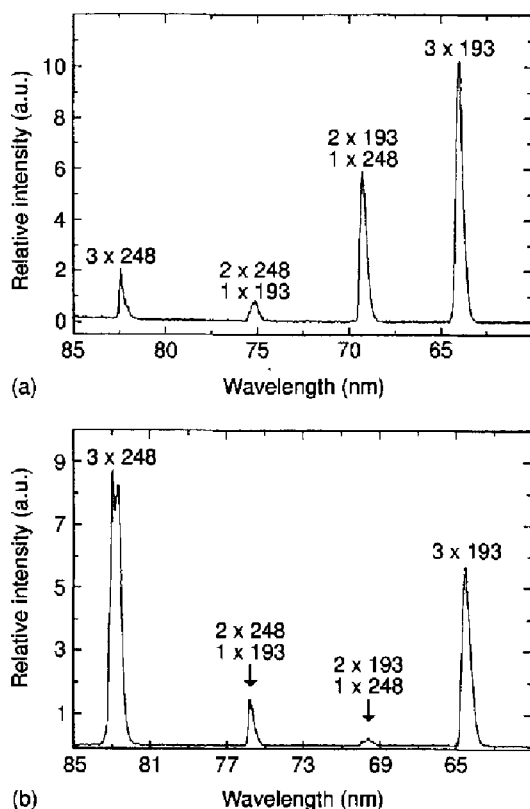


Figure 13 Third-order mixing spectrum of KrF (248 nm) and ArF (193 nm) radiation in H₂ (a) and argon (b). Pump intensities $\sim 10^{15}$ W cm⁻². The relative intensity scales are comparable.

generation (Fig. 7), except that two laser fields have to be overlapped spatially and temporally in the nonlinear medium, which was accomplished by focusing one beam through a dichroic mirror and by a variable delay line.

Figure 13 shows as an example third-order mixing of KrF (248 nm) and ArF (193 nm) short pulses in argon and molecular hydrogen at comparable focused intensities (10^{15} W cm⁻²). Here, the influence of multiphoton resonances can be observed. Both the third harmonic of ArF (193 nm) and the 2×193 nm + 248 nm mixing signals are strongly increased in the case of hydrogen compared to argon, whereas the third harmonic of the KrF laser is much stronger in argon compared to hydrogen. This can be explained by a strong two-photon resonance for the 193 nm radiation in molecular hydrogen ($X^1\Sigma_g^+(\nu=0)$ -E, $F^1\Sigma_g^+(\nu=2)$) [29] and a three-photon resonance enhancement for the 248 nm radiation in argon ($3p^6\ ^1S_0$ -4d [3/2]⁰) [30].

In Fig. 14 all fifth-order sum mixing signals of ArF and KrF laser radiation and in Fig. 15 seventh-order mixing signals of KrF radiation with 496 nm radiation internally generated in the KrF system (see Fig. 2) are shown. The spectra clearly indicate that tunable XUV radiation can be generated if one of the mixing fields is tunable. The KrF 248 nm/496 nm mixing signals could be detected down to about 10 μ J of the 496 nm radiation at intensities around 10^{12} W cm⁻². In order to realize broadly tunable XUV radiation by this mixing concept, a tunable short-pulse source with energies of at least several hundred microjoules, allowing intensities of more than 10^{13} W cm⁻², is needed. For this, we have developed an optical parametric

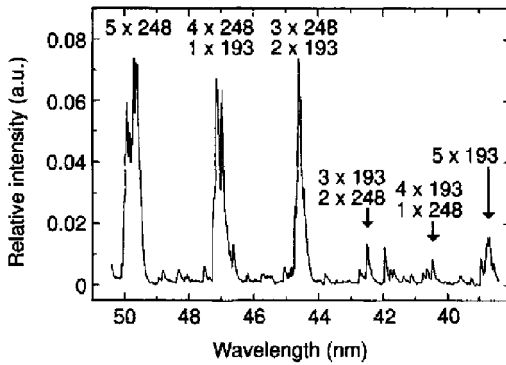


Figure 14 Fifth-order harmonic and mixing spectrum of KrF (248 nm) and ArF (193 nm) radiation in argon. Pump intensities $\sim 10^{15} \text{ W cm}^{-2}$. Scale comparable to relative scale of Fig. 13. The modulation of the intensity of the signals is mainly due to pulse-to-pulse fluctuations of the lasers (no single-shot spectrum).

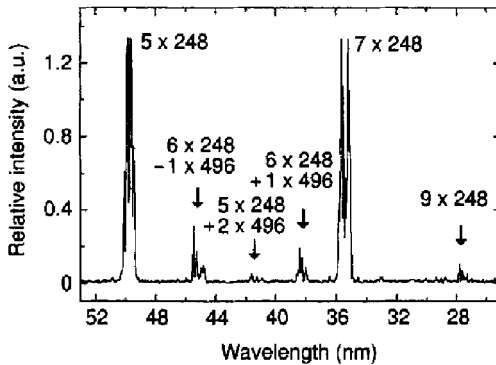


Figure 15 Seventh-order harmonic and mixing spectrum of 248 nm ($\sim 5 \times 10^{15} \text{ W cm}^{-2}$) and 496 nm ($\sim 10^{13} \text{ W cm}^{-2}$) radiation in helium. Scale comparable to scales of Figs 13 and 14. The modulation of the intensity of the signals is mainly due to pulse-to-pulse fluctuations of the lasers (no single-shot spectrum).

generator–amplifier (OPG) source pumped by frequency-doubled Ti:sapphire laser radiation and have mixed radiation from this source with the fundamental of the Ti:sapphire system (Fig. 3).

The setup is shown in Fig. 16. With about 5–10 mJ (~ 200 fs) at 405 nm, some 300–400 μJ (600 fs) of OPG radiation, so far tunable in the range 520–650 nm, could be generated. With this tunable radiation, frequency mixing signals ($2n\omega_p \pm \omega_{\text{OPG}}$; in first order of the OPG radiation) could be resolved up to wavelengths of 46 nm in xenon and 37 nm in argon, as shown in Fig. 17. For xenon also weak signals at $(2n + 1)\omega_p \pm 2\omega_{\text{OPG}}$ (second order of the OPG radiation) could be detected [31]. Figure 18 shows in more detail a detuning of the ninth-order sum mixing signal in xenon around 87 nm. As discussed in [31], with the first- and second-order OPG mixing process and the potential tuning range of the OPG signal wave (about 480 nm to 800 nm), practically the whole range between two subsequent harmonics of the Ti:sapphire radiation can be covered, so that in principle tunable short-pulse radiation down to the highest-order harmonics in neon (~ 10 nm) should also be possible if the intensity of the OPG can be further increased by increasing the output energy and by improving the beam quality.

6. Conclusions

In recent years, nonperturbative high-order harmonic generation has been rigorously investigated, and short wavelengths as well as good output powers have been achieved. Recently

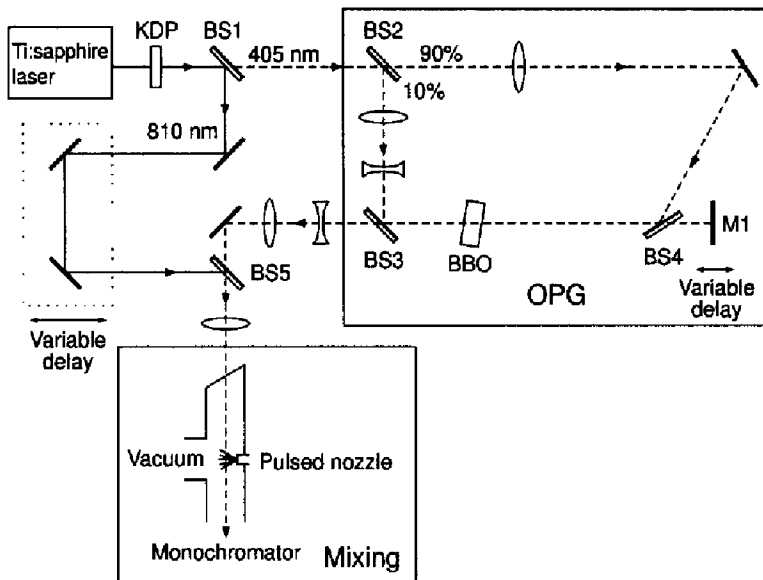


Figure 16 Setup for high-order frequency mixing of Ti:sapphire (810 nm) radiation with tunable radiation from an optical parametric generator–amplifier (OPG). Pump radiation at 405 nm is used to generate parametric fluorescence in BBO. At mirror M1 back-reflected fluorescence is used as seed radiation in a second amplification pass through the BBO crystal.

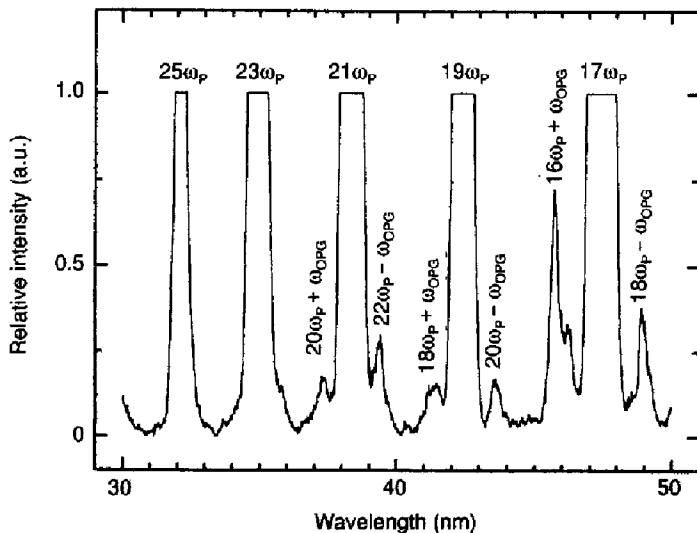


Figure 17 Part of the high-order harmonic and mixing spectrum of Ti:sapphire (ω_p 810 nm, $\sim 10^{15}$ W cm $^{-2}$) and OPG (ω_{OPG} 520–650 nm, ≤ 400 μ J) radiation in argon.

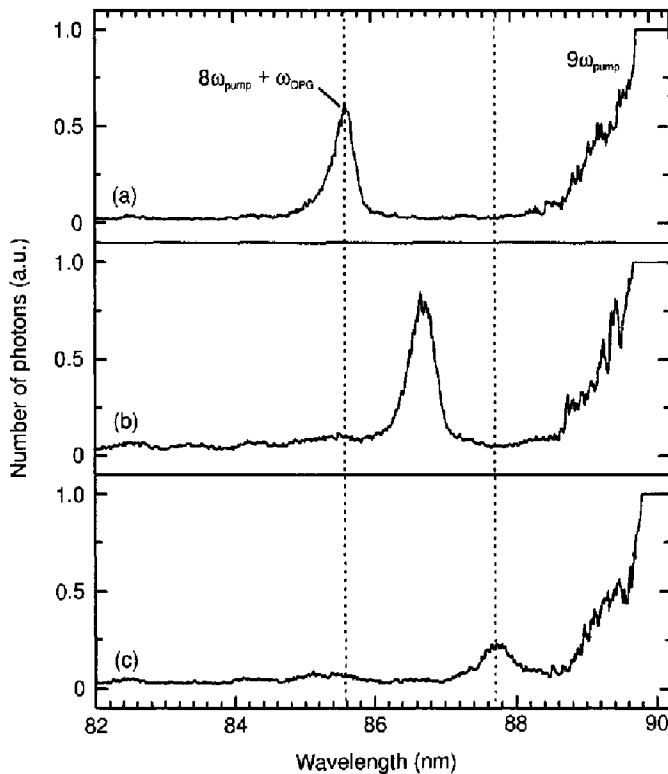


Figure 18 Demonstration of tunability of the $8\omega_{\text{pump}} + \omega_{\text{OPG}}$ mixing signal in the vicinity of the ninth-order Ti:sapphire harmonic for xenon as nonlinear material. The OPG radiation has been tuned to three different wavelengths: (a) 545 nm; (b) 590 nm; (c) 640 nm.

first applications of these sources have also been reported or planned in spectroscopy [32] and as seed radiation in x-ray laser research.

In this paper low- and higher-order mixing schemes have been described that allow tunability in principle down to the shortest wavelengths achieved with the harmonics. This will stimulate further applications.

By four-wave mixing in xenon, tunable short-pulse VUV radiation with peak powers approaching the gigawatt range has been realized, which should allow novel nonlinear experiments.

For the higher-order mixing process, the power generated is still small, but can surely be significantly improved by higher pump intensities and the optimization of focusing and phase-matching conditions. For two-colour mixing experiments additional degrees of freedom for influencing the process exist. In the first $\omega-2\omega$ mixing experiments we investigated the intensities of the mixing signals and the position of the cutoff for linear and circular polarizations and different relative orientations of the two fields [33].

Finally, considering effort and progress in the realization of compact high-power laser systems, it can be expected that the generation of coherent XUV radiation by nonlinear optics will develop into a standard laboratory tool.

Acknowledgements

The authors thank H. Jacobs for valuable help in preparing the manuscript and the Deutsche Forschungsgemeinschaft for financial support of the project.

References

1. *Proceedings of the 3rd International Colloquium on X-Ray Lasers 1992*, Schliersee, Germany, 1992, edited by E. E. Fill, Institute of Physics Conference Series **125**.
2. R. C. ELTON, *X-Ray Lasers* (Academic Press, New York, 1990).
3. J. REINTJES, C. Y. SHI and R. C. ECKARDT, *IEEE J. Quantum Electron.* **QE-14** (1978) 581.
4. C. E. M. STRAUSS and D. J. FUNK, *Opt. Lett.* **16** (1991) 1192.
5. Y. HIRAKAWA, T. OKADA, M. MEODA and K. MURAOKA, *Opt. Commun.* **84** (1991) 365.
6. G. HILBER, A. LAGO and R. WALLENSTEIN, *J. Opt. Soc. Am. B* **4** (1987) 1753.
7. P. C. HINNEN, W. HOGERVORST, S. STOLTE and W. UBACHS, *Appl. Phys. B* **59** (1994) 307.
8. K. S. E. EIKEMA, W. UBACHS, W. VASSEN and W. HOGERVORST, *Phys. Rev. Lett.* **68** (1993) 1690.
9. A. L'HUILLIER and PH. BALCOU, *Phys. Rev. Lett.* **70** (1993) 774.
10. J. J. MACKLIN, J. D. KMETEC and C. L. GORDON, *Phys. Rev. Lett.* **70** (1993) 766.
11. K. MIYAZAKI and H. SAKAI, *J. Phys. B: At. Mol. Opt. Phys.* **25** (1992) L83.
12. N. SARUKURA, K. HATA, T. ADACHI, R. NODOMI, M. WATANABE and S. WATANABE, *Phys. Rev. A* **43** (1991) 1669.
13. M. D. PERRY and G. MOUROU, *Science* **264** (1994) 917.
14. A. TUNNERMANN, K. MOSSAVI and B. WELLEGEHAUSEN, *Phys. Rev. A* **46** (1992) 2707.
15. S. SZATMÁRI and F. P. SCHÄFER, *Opt. Commun.* **68** (1988) 196.
16. G. ALMÁSI, S. SZATMÁRI and P. SIMON, *Opt. Commun.* **88** (1992) 231.
17. A. TUNNERMANN, C. MOMMA, K. MOSSAVI, C. WINDOLPH and B. WELLEGEHAUSEN, *IEEE J. Quantum Electron.* **QE-29** (1993) 1233.
18. C. MOMMA, H. EICHMANN, K. MOSSAVI, M. FEUERHAKE and B. WELLEGEHAUSEN, *Proceedings of the VIIIth International Symposium on Ultrafast Processes in Spectroscopy*, Vilnius, Lithuania, 1993, p. 339.
19. C. MOMMA, H. EICHMANN, H. JACOBS, A. TUNNERMANN, H. WELLING and B. WELLEGEHAUSEN, *Opt. Lett.* **18** (1993) 516.
20. C. MOMMA, H. EICHMANN, A. TUNNERMANN, P. SIMON, G. MAROWSKY and B. WELLEGEHAUSEN, *Opt. Lett.* **18** (1993) 1180.
21. J. L. KRAUSE, K. J. SCHAFER and K. C. KULANDER, *Phys. Rev. Lett.* **68** (1992) 3535.
22. C.-G. WAHLSTROM, J. LAKSSON, A. PERSSON, *et al.*, *Phys. Rev. A* **48** (1993) 4709.
23. W. BECKER, S. LONG and J. K. McIVER, *Phys. Rev. A* **50** (1994) 1540.
24. A. L'HUILLIER, M. LEWENSTEIN, P. SALIÈRES, *et al.*, *Phys. Rev. A* **48** (1993) R3433.
25. T. SRINIVASAN, K. BOYER, H. EGGER, *et al.*, *Picosecond Phenomena III*, edited by K. B. Eisenthal, R. M. Hochstrasser, W. Kaiser and A. Laubereau (*Chemical Physics* **23**; Springer, Berlin, 1982).
26. L. V. KELDYSH, *Sov. Phys. JETP* **20** (1965) 1307.
27. K. KONDO, N. SARUKURA, K. SAJIKI and S. WATANABE, *Phys. Rev. A* **47** (1993) R2480.
28. M. H. KEY, *Nature* **316** (1985) 314.
29. H. PUMMER, T. SRINIVASAN, H. EGGER, T. S. LUK and C. K. RHODES, *Opt. Lett.* **7** (1982) 93.
30. R. L. KELLY, *J. Phys. Chem. Ref. Data* **16** (Supplement 1) (1987) 42.
31. H. EICHMANN, S. MEYER, K. RIEPL, C. MOMMA and B. WELLEGEHAUSEN, *Phys. Rev. A* **50** (1994) R2834.
32. R. HAIGHT and P. F. SEIDLER, *Appl. Phys. Lett.* **65** (1994) 517.
33. H. EICHMANN, A. EGBERT, S. NOLTE, *et al.*, *Phys. Rev. A* **51** (1995) R3414.